Synthesis and Swelling Characteristics of a pH-Responsive Guar Gum-*g*-Poly(Sodium Acrylate)/Medicinal Stone Superabsorbent Composite

Naihua Zhai,[1,2] **Wenbo Wang,**[1,2] **Aiqin Wang**[1]
[1]*Center of Eco-material and Green Chemistry, Lanzhou Institute of Chemical Physics, Chinese Academy of Sciences, Lanzhou, People's Republic of China*

[2]*Graduate University of the Chinese Academy of Sciences, Beijing, People's Republic of China*

A series of pH-responsive superabsorbent composites were synthesized by the free-radical grafting copolymerization of natural guar gum (GG), partially neutralized acrylic acid (NaA), and medicinal stone (MS) using ammonium persulfate (APS) as the initiator and *N,N′*-methylene-*bis*-acrylamide (MBA) as the crosslinker. The structure, surface morphologies, and thermal stability of the developed composites were characterized by FTIR spectra, SEM, and TGA techniques, respectively. The effects of various saline, surfactant, and dye solutions on swelling properties were investigated, and the pH-responsivity was also evaluated. Results indicated that NaA had been grafted onto GG macromolecular chains and MS participated in the polymerization reaction. The incorporation of MS obviously improved the surface structure, thermal stability, water absorption capacity, and rate. Multivalent saline, cationic surfactant, and dye showed more remarkable effect on the water absorption than did monovalent or anionic ones. The composites showed excellent responsive properties and reversible On–Off switching characteristics in various pH buffer solutions, which provided great possibility to extend the application domain of the superabsorbent composites. POLYM. COMPOS., 32:210–218, 2011. © 2010 Society of Plastics Engineers

INTRODUCTION

Composite of organic polymers with inorganic clay minerals has long been the subject of great interest in scientific research and industrial applications because the incorporation of clay minerals may reduce production cost and improve the performance of material [1–3]. Superabsorbents are particular functional material with unique 3-D hydrophilic network structure and highly water-swellable characteristic, which have attracted continuous attention and found extensive application in various fields, such as hygienic products [4], agriculture [5, 6], wastewater treatment [7–9], catalyst supports [10], and drug-delivery systems [11]. However, the conventional superabsorbents are based on fully organic petroleum-based polymers with high-production cost and poor environmental-friendly properties [12]. Thus, new types of superabsorbents derived from naturally available raw materials have long been desired.

In recent years, polysaccharide-based materials as a potential substitute for nondegradable materials have received increasing attention owing to their unique low-cost, renewable, biodegradable, nontoxic, and biocompatible characteristics [13, 14]. Among them, the composites of polysaccharides with easy available, abundant, and environmentally friendly inorganic clay minerals are especially potential because they exhibited excellent hybrid performance, and such materials have been honored as the material families of "in greening the 21st century materials world" [15]. Thus far, some natural polysaccharides such as starch [16, 17], cellulose [18], chitosan [19, 20], gelatin [21], alginate [22], dextrin [23], cashew gum [24], and carrageenan [25] have been used as matrix polymer to develop new types of ecofriendly superabsorbent materials, and the resultant materials also exhibited ameliorative properties.

Guar gum (GG) is derived from the seeds of guar plant *Cyanaposis tetragonolobus* (Leguminosae). It is a natural nonionic branched polysaccharide with β-D-mannopyranosyl units linked (1-4) with single membered α-D-galactopyranosyl units occurring as side branches. GG and its derivatives have been used in many fields (e.g., thickening agent, ion exchange resin, and dispersing agent). Me-

Correspondence to: A. Wang; e-mail: aqwang@licp.cas.cn
Contract grant sponsor: Western Action Project of CAS; contract grant number: KGCX2-YW-501.
Contract grant sponsor: Project of the Ministry of Science and Technology, P. R. China; contract grant numbers: 2006AA03Z0454 and 2006AA100215.
DOI 10.1002/pc.21017
Published online in Wiley Online Library (wileyonlinelibrary.com)
© 2010 Society of Plastics Engineers

dicinal stone (MS) is a special igneous rock composed of silicic acid, alumina oxide, and more than 50 kinds of constant and trace elements. The main chemical composition of MS is aluminum metasilicate including $KAlSi_3O_8$, $NaAlSi_3O_8$, $CaAl_2Si_2O_8$, $MgAl_2Si_2O_8$, and $FeAl_2Si_2O_8$. In such a structure, silica (SiO_2) presents regular tetrahedron with a [SiO_4] configuration and shows a three-dimensional stereo-structure. In a part of its structure, aluminum coordinates through oxobridging. By virtue of the unique porousness, multicomponent characteristic, biological activity, and safety, MS has been extensively applied in food science, medicine, daily chemical industry, environmental sanitation, and wastewater treatment [26]. However, rare information regards on the application of MS as an inorganic additive of superabsorbent composites. So, the chemical composite of GG and MS was expected to derive superabsorbent materials with improved network structure and comprehensive performance.

In this work, the novel guar gum-*g*-poly(sodium acrylate)/medicinal stone (GG-*g*-PNaA/MS) superabsorbent composites were prepared by the grafting copolymerization of GG and NaA in the presence of MS micropowder. The developed composites were characterized by Fourier transform infrared (FTIR) spectra, scanning electron microscopy (SEM), and thermogravimetric analysis (TGA). The effects of MS content on water absorption and swelling kinetics were investigated. Also, the pH-responsivity and the swelling behaviors of the composites in various saline, surfactant, and dye solutions were evaluated systematically.

EXPERIMENTAL

Materials

Guar gum (GG, food grade, number average molecular weight 220,000) was from Wuhan Tianyuan Biology Co., China. Acrylic acid (AA, chemically pure, Shanghai Shanpu Chemical Factory, Shanghai, China) was distilled under reduced pressure before use. Medicinal stone (MS) micropowder (Chinese M-Stone Development CO., Ltd, NaiMan, Inner Mongolia, China) was milled and passed through a 320-mesh screen (< 46 μm) before use. The main chemical composition of MS is SiO_2, 68.89%; Al_2O_3, 14.06%; Fe_2O_3, 3.61%; K_2O, 3.18%; Na_2O, 4.86%; CaO, 1.33%; MgO, 2.59%. Ammonium persulfate (APS, analytical grade, Xi'an Chemical Reagent Factory, China) and *N,N′*-methylenebisacrylamide (MBA, Chemically Pure, Shanghai Chemical Reagent Corp., China) was used as received. Dodecyltrimethylammonium bromide (DTAB, Beijing Chemical Reagents Company, China) was used as purchased. Sodium dodecylsulfate (SDS, Chemically Pure) was purchased from Beijing Chemical Reagents Company (China). Congo Red and Methylene Blue was purchased from Alfa Aesar A Johnson Matthey Company. All other reagents used were of analytical grade, and all solutions were prepared with distilled water.

Preparation of GG-g-PNaA/MS Superabsorbent Composites

GG (1.20 g) was dispersed in 34 mL of NaOH solution (0.067 M, pH 12.5) in a 250-mL four-necked flask equipped with a mechanical stirrer, a thermometer, a reflux condenser and a nitrogen line, and the dispersion was heated with an oil bath to 60°C and kept for 1 h to form a colloidal slurry. Afterward, 5 mL of the aqueous solution of initiator APS (0.1008 g) was added dropwise to the reaction flask under continuous stirring and kept at 60°C for 10 min to generate radicals. 7.2 g of acrylic acid was neutralized using 8.0 mL of 8.5 M NaOH to achieve a total neutralization degree of 70% (under consideration of the 34 mL of 0.067 M NaOH solution used to disperse GG), and then crosslinker MBA (21.6 mg) and MS powder (0.95 g) were added under magnetic stirring to form a uniform dispersion. After cooling the reactant to 50°C, the dispersion was added to the reaction flask, and temperature was slowly risen to 70°C and kept for 3 h to complete polymerization. Continuous purging of nitrogen was used throughout the reaction period. The obtained gel products were dried to a constant mass at 70°C and ground and passed through 40–80 mesh sieve (180–380 μm). GG-*g*-PNaA superabsorbent hydrogel was prepared by a similar procedure except without the addition of MS.

Measurements of Equilibrium Water Absorption and Swelling Kinetics

A 0.05 g of dry superabsorbent particle with the size of 180–380 μm was soaked in excessive aqueous solution at room temperature for 4 h to reach swelling equilibrium. The swollen samples were filtered using a 100-mesh screen and then drain on the sieve for 10 min to remove the redundant water. After weighing the swollen samples, the equilibrium water absorption of the superabsorbent was calculated using:

$$Q_{eq} = (w_s - w_d)/w_d. \quad (1)$$

Q_{eq} is the equilibrium water absorption calculated as grams of water per gram of the sample, which are averages of three measurements; w_d and w_s are the weights of the dry sample and water-swollen sample, respectively.

Swelling kinetics of superabsorbents in distilled water was measured by the following procedure: 0.05-g samples were contacted with 200 mL solution. The swollen gels were filtered using a sieve after different time periods (1, 3, 5, 8, 10, 15, 20, 30, 60, and 120 min), and the water absorption of superabsorbents at a given time can be measured by weighing the swollen and dry samples, and calculated according to Eq. *1*. In all cases, three parallel samples were used, and the averages were reported in this article.

Evaluation of pH-Responsivity

The buffer solutions with various pH values were prepared by combining KH_2PO_4, K_2HPO_4, H_3PO_4, and

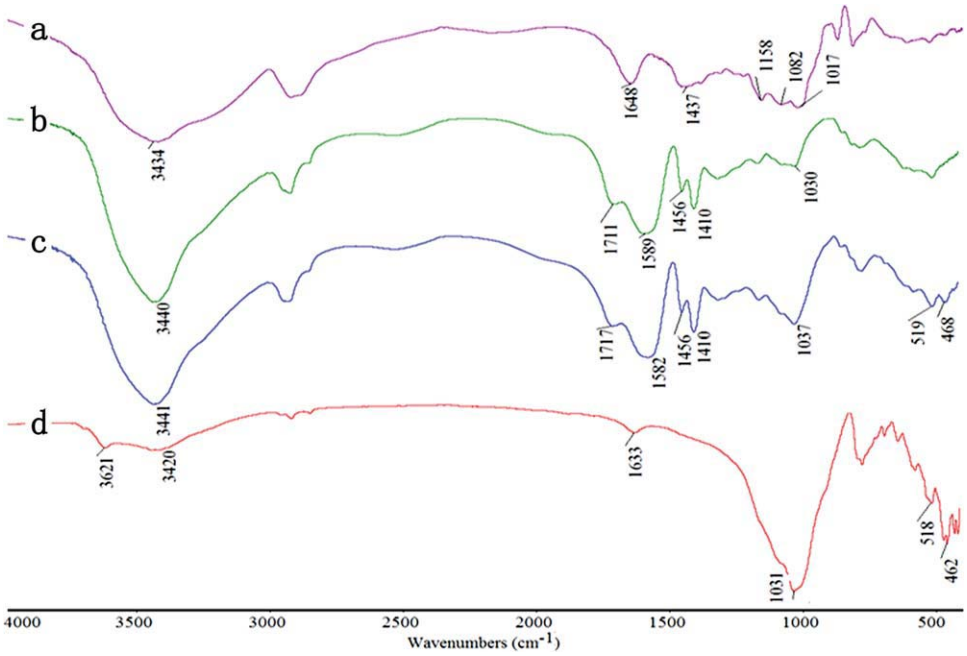

FIG. 1. FTIR spectra of (a) GG, (b) GG-*g*-PNaA, (c) GG-*g*-PNaA/MS (10 wt%), and (d) MS. [Color figure can be viewed in the online issue, which is available at wileyonlinelibrary.com.]

NaOH solution properly, and the pH values were determined by a pH meter (DELTA-320). Ionic strengths of all the buffer solutions were controlled to 0.1 M using NaCl solution. The equilibrium water absorption (Q_{eq}) in various pH buffer solutions was measured by a method similar to that in distilled water. The pH-reversibility of the superabsorbent composites was investigated in terms of their swelling and deswelling in pH buffer solution of phosphate between pH 2.0 and 7.2. Typically, the sample particle (0.05 g, 180–380 μm) was placed in a 100-mesh sieve and adequately contacted with pH 2.0 buffer solution until reaching equilibrium. Then, the swollen samples were soaked in pH 7.2 buffer solution for set time intervals. Finally, the swollen samples were filtered, weighed, and then the water absorption at a given moment was calculated according to the mass change of samples before and after swelling. The consecutive time interval is 15 min for each cycle, and the same procedure was repeated for five cycles. After every measurement, each solution was renewed.

Characterizations

FTIR spectra were recorded on a Nicolet NEXUS FTIR spectrometer in 4000–400 cm^{-1} region using KBr platelets. The sample after swelling in dye solution was fully washed and dried before FTIR determination. The morphologies of the samples were examined using a JSM-5600LV SEM instrument (JEOL) after coating the sample with gold film. Thermal stability of samples was studied on a Perkin-Elmer TGA-7 thermogravimetric analyzer (Perkin-Elmer Cetus Instruments, Norwalk, CT), with a temperature range of 25–800°C at a heating rate of 10°C/min using dry nitrogen purge at a flow rate of 50 mL/min. The samples were dried at 100°C for 4 h before determining TG curves.

RESULTS AND DISCUSSION

FTIR Spectra Analysis

As shown in Fig. 1, the characteristic absorption bands of GG at 1,017, 1,082, and 1,158 cm^{-1} (the stretching vibration of C—O(H)) and the band at 1,648 cm^{-1} (bending vibration of —OH groups) almost disappeared and the new bands at 1,711 cm^{-1} for GG-*g*-PNaA and 1,717 cm^{-1} for GG-*g*-PNaA/MS (C=O asymmetric stretching vibration of —COOH), at 1,589 cm^{-1} for GG-*g*-PNaA and 1,582 cm^{-1} for GG-*g*-PNaA/MS (asymmetric stretching vibration of $—COO^-$ groups), at 1,456 and 1,410 cm^{-1} (symmetric stretching of $—COO^-$ groups) appeared after grafting copolymerization with NaA (Fig. 1a–c). This indicates that NaA had grafted onto the macromolecular chains of GG. The stretching vibration of (Si)O—H at 3621 cm^{-1} disappeared in the spectrum of GG-*g*-PNaA/MS (Fig. 1c and d). The Si—O stretching vibration of MS at 1,031 cm^{-1} shift to 1,037 cm^{-1} after forming composite, but its intensity was obviously weakened. The Si—O bending vibration can be observed in the spectrum of GG-*g*-PNaA/MS with weakened intensity. This information gives direct evidence that MS participated in the graft copolymerization reaction through its active silanol groups [27, 28].

 DOI 10.1002/pc

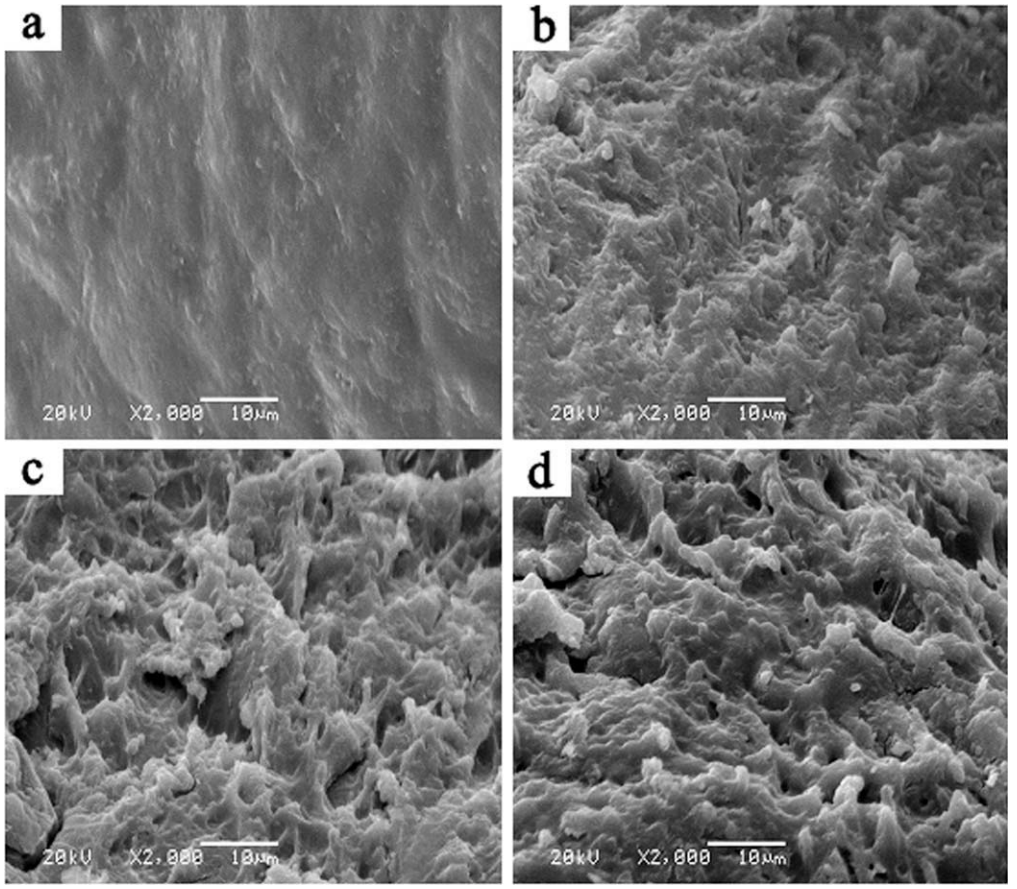

FIG. 2. SEM micrographs of (a) GG-*g*-PNaA, (b) GG-*g*-PNaA/MS (10 wt%), (c) GG-*g*-PNaA/MS (20 wt%), and (d) GG-*g*-PNaA/MS (30 wt%).

SEM Analysis

Figure 2 depicted the SEM micrographs of the superabsorbent composites containing various amounts of MS. It can be observed that GG-*g*-PNaA only exhibit a smooth and dense surface (Fig. 2a), while the superabsorbent composites containing MS show a correspondingly coarse, loose and undulant surface (Fig. 2b–d). The surface roughness of GG-*g*-PNaA/MS increased with increasing the content of MS, which implies that introduction of MS is favorable to improve the surface structure of the resultant composite. Furthermore, it can be obviously observed that MS is uniformly dispersed and almost embedded within the GG-*g*-PNaA matrix without the flocculation of MS particles, indicating that a homogeneous composition of MS with the matrix network was formed.

TGA

Figure 3 presents the TGA curves of GG-*g*-PNaA hydrogel and GG-*g*-PNaA/MS (10 wt%) superabsorbent composite. It is obvious that both GG-*g*-PNaA and GG-*g*-PNaA/MS (10 wt%) shows a three-stage thermal decomposition, and the weight-loss rate of GG-*g*-PNaA is faster than that of GG-*g*-PNaA/MS. The weight loss below 331°C for GG-*g*-PNaA and 314°C for GG-*g*-PNaA/MS can be ascribed to the dehydration of saccharide rings, the breaking of C—O—C bonds in the chain of GG, and the elimination of the water molecule from the two neighboring carboxylic groups of the grafted chains due to the formation of anhydride [29]. The successive weight losses from 331 to 429°C for GG-*g*-PNaA and from 314 to 431°C for GG-*g*-PNaA/MS can be attributed to the destruction of carboxylic groups and CO_2 evolution as well as main-chain scission [30]. The weight losses from 429 to 498°C for GG-*g*-PNaA and from 431 to 496°C for GG-*g*-PNaA/MS are due to the breakage of PNaA chains and the destruction of the crosslinked network. Comparing with GG-*g*-PNaA, GG-*g*-PNaA/MS shows lower total weight loss, and this reveals that the incorporation of MS enhanced the thermal stability of the superabsorbent composite.

Effect of MS Content on Water Absorption

Content of MS in the composite decided its composition and structure, and certainly affected its swelling properties. As shown in Fig. 4, the water absorption of the composite greatly increased with increasing MS content until a maximum absorption (632 g/g) was achieved at 10 wt%. Compared with the MS-free sample, the water absorption of the composite with 10 wt% MS increased

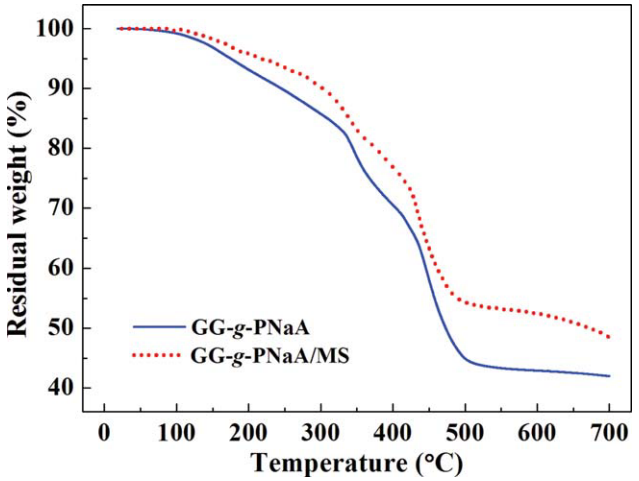

FIG. 3. TGA curves of (a) GG-*g*-PNaA, and (b) GG-*g*-PNaA/MS (10 wt%) superabsorbent composite. [Color figure can be viewed in the online issue, which is available at wileyonlinelibrary.com.]

by 96%. The great improvement of water absorption can be attributed to the fact that (i) MS can ionize and release lots of metal cations as contacting with water [26], which increased the concentration of electrolyte in interior gel network and enhanced the osmotic pressure difference between gel network and swelling media, and so the water absorption can be improved; (ii) MS may participate in polymerization reaction. On the one hand, the polymer network can be regularly formed; on the other hand, the incorporation of rigid MS particles prevented intertwining of grafted polymeric chains and weakened the hydrogen-bonding interaction among hydrophilic groups. As a result, the degree of physical crosslinking was decreased, and the water absorption was improved; (iii) ionization of MS may generate $[—SiO]^-$ groups [26], which can repulse with the negatively charged graft polymer chains and facilitate the expansion of gel network. This factor is responsible for the improvement of water absorption.

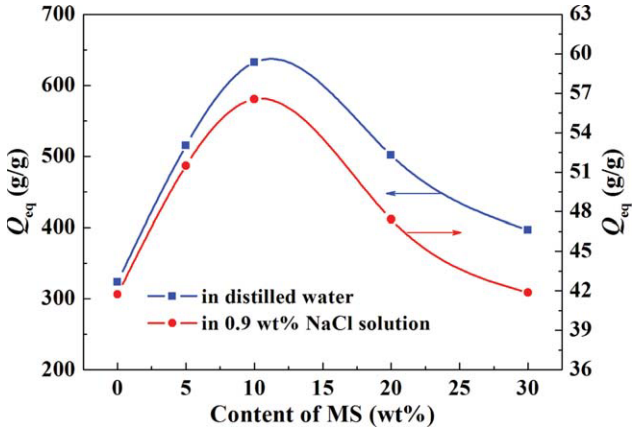

FIG. 4. Variation of water absorption for the GG-*g*-PNaA/MS superabsorbent composite with MS content. [Color figure can be viewed in the online issue, which is available at wileyonlinelibrary.com.]

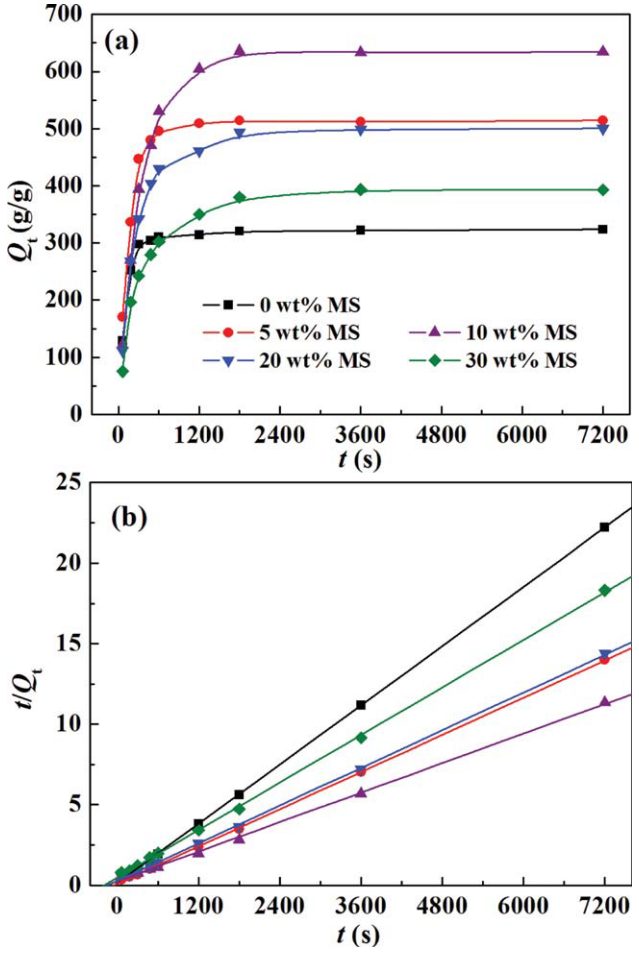

FIG. 5. (a) Swelling kinetics curves of the superabsorbents with various contents of MS, and (b) the plots of t/Q_t against t for each superabsorbent. [Color figure can be viewed in the online issue, which is available at wileyonlinelibrary.com.]

It can also be observed that the water absorption decreased when the addition amount of MS exceeded 10 wt%. This is because that the excess MS is physically filled in the gel network. Consequently, the network voids for holding water was obstructed and the hydrophilicity of the composite was decreased. As a result, the water absorption decreased with the increase of MS content above 10 wt%. A similar tendency was observed for poly(acrylic acid-*co*-*N*-acryloylmorpholine)/attapulgite superabsorbent composite [31].

Swelling Kinetics

Beside swelling capability, swelling rate is also an important index of evaluating the performance of superabsorbents. Figure 5a represents the kinetic swelling curves of the superabsorbents. The water absorption rapidly increased with prolonging contact time at initial 600 s, and then the swelling curves become flatter until equilibrium was reached. For evaluating the effect of MS content

DOI 10.1002/pc

TABLE 1. Swelling kinetic parameters of GG-*g*-PNaA and GG-*g*-PNaA/MS.

Samples	Q_∞ (g/g)	K_{is} (s)	R
GG-*g*-PNaA	326	7.1628	0.9999
GG-*g*-PNaA/MS (5 wt%)	521	9.1141	0.9999
GG-*g*-PNaA/MS (10 wt%)	654	3.7655	0.9995
GG-*g*-PNaA/MS (20 wt%)	513	3.6677	0.9998
GG-*g*-PNaA/MS (30 wt%)	407	2.0602	0.9998

on swelling rate, the Schott's pseudosecond-order kinetics model was introduced and expressed by [32]:

$$t/Q_t = 1/K_{is} + (1/Q_\infty)t. \quad 2$$

Q_t is the water absorption at a given swelling time t (s); Q_∞ (g/g) is the power parameter, denoting the theoretical equilibrium water absorption; K_{is} is the initial swelling rate constant (g/g·s). It can be seen from Fig. 5b, the plots of t/Q_t versus t gives perfect straight line with good linear correlation coefficient, indicating that the pseudosecond-order model is suitable for evaluating the swelling kinetics of the composite. The values of K_{is} and Q_∞ can be determined by fitting experimental data using Eq. *2* and calculated by the slope and intercept of the straight lines (Table 1). According to the obtained values of K_{is} and Q_∞ for each superabsorbent, it can be concluded that the initial swelling rate decreased in the order: GG-*g*-PNaA/MS (5 wt%) > GG-*g*-PNaA > GG-*g*-PNaA/MS (10 wt%) > GG-*g*-PNaA/MS (20 wt%) > GG-*g*-PNaA/MS (30 wt%). This gives direct revelation that the compounding of moderate amount of MS into GG-*g*-PNaA network facilitates to improve its swelling rate.

pH-Responsive Properties

Figure 6a depicts the swelling behaviors of GG-*g*-PNaA/MS composites in various pH buffer solutions (0.1 M). It can be noticed that the water absorption of the composites is low at acidic condition (pH < 4), but it sharply increased and almost keeps constant in the range of pH from 6 to 13 when the pH > 4. This phenomenon presents a remarkable pH-responsive characteristic of the composites and is ascribed to the following reason. The composite is an anionic polymer with large amounts of —COO^- and —COOH groups. In acidic media, —COO^- groups converted to —COOH groups, the number of —COO^- groups rapidly decreased and the amount of —COOH groups greatly increased [33]. As a result, the hydrogen bonding interaction among hydrophilic groups such as —OH and —COOH strengthened, the degree of physical crosslinking increased and the repulsion among polymer chains was weakened. Thus, the swelling of superabsorbent at low pH was restrained. As the external pH increased, the contrary process occurred. The hydrogen bonding interaction was broken, and the electrostatic repulsion among polymer chains was increased because of the rapid increase in the number of negatively charged —COO^- groups, and so the polymer network tends to swell more. For evaluating the reversibility of pH response, the typical swelling–deswelling properties were determined in 0.1 M buffer solution of phosphate between pH 2 and 7.2 (Fig. 6b). The composite achieved higher absorption at pH 7.2, but the swollen gel rapidly shrinks after being soaked in pH 2 buffer solutions and switched between On (at pH 7.2) and Off (at pH 2) states. After five On–Off cycles, the composites still have better responsivity, indicating that the responsive behaviors are reversible.

Effects of Saline Solution on Water Absorption

The swelling properties of superabsorbent in saline solution are especially significant to its practical application in each field. In this section, the effects of saline solutions

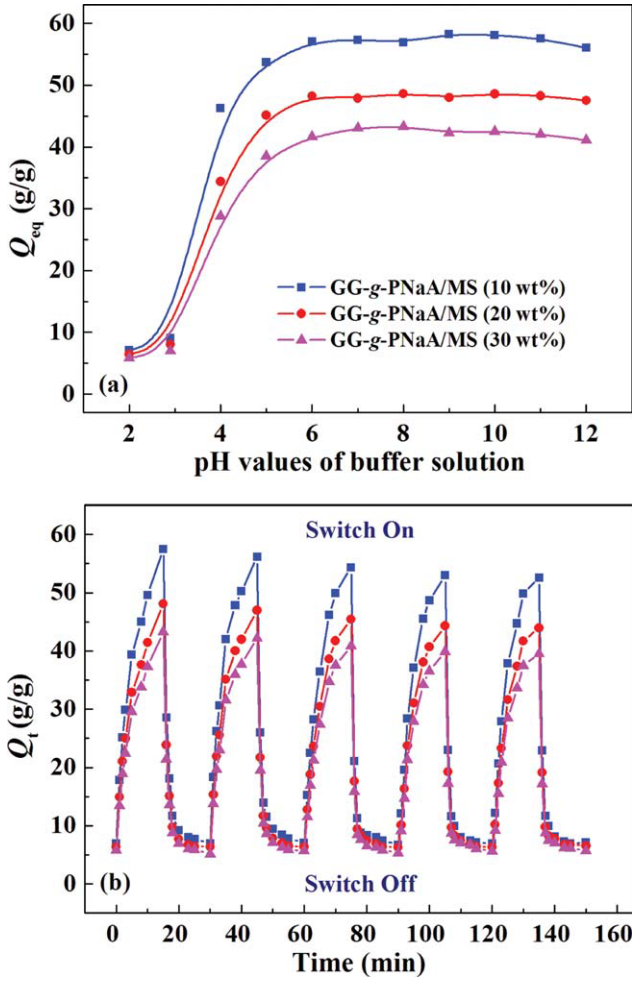

FIG. 6. (a) Variation of water absorption for GG-*g*-PNaA/MS (10, 20, and 30 wt%) composites at the buffer solution of various pH values, and (b) the On–Off switching behavior of the composite as reversible pulsatile swelling (pH 7.2) and deswelling (pH 2.0). [Color figure can be viewed in the online issue, which is available at wileyonlinelibrary.com.]

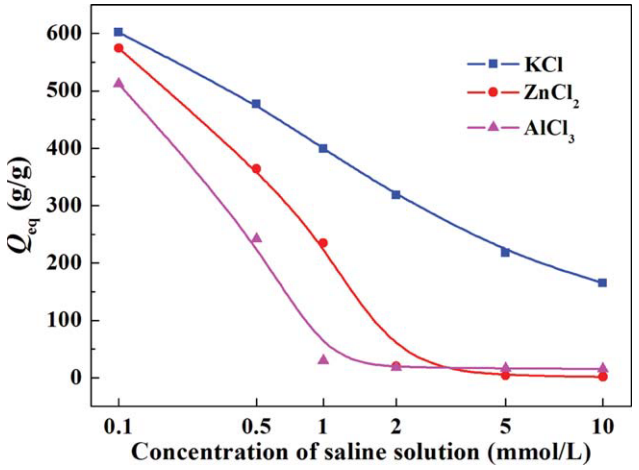

FIG. 7. Effect of saline solution on the water absorption. [Color figure can be viewed in the online issue, which is available at wileyonlinelibrary.com.]

with different cations (K^+, Zn^{2+}, and Al^{3+}) and common anion (Cl^-) on the water absorption of GG-*g*-PNaA/MS (10 wt%) superabsorbent composite was investigated (see Fig. 7). The water absorption degreased with increasing the concentration of external saline solution, and the deswelling behavior is more obvious in multivalence saline solutions than in monovalent saline solution. At higher concentration, the water absorption of the composite is almost close to zero in $ZnCl_2$ and $AlCl_3$ solution, but certain absorption (165 g/g) can be achieved in KCl solution. As described previously [34], the deswelling of ionic superabsorbents to monovalent saline is mainly attributed to the reduction of osmotic pressure difference between the gel networks and the saline-containing medium as well as the screening effect of cations (e.g., Na^+, K^+) on the negative charge of polymer chains. However, some additional action occurred in multivalent saline solution along with the decrease of osmotic pressure difference and the increase of screening effect because the ionic sites of superabsorbents may complex with multivalent cations, and also the $—COO^-$ groups may be protonated in $AlCl_3$ solution (pH 3.7 at 10 mmol/L). This reduced the negative charges in polymeric chains and produces denser crosslinking network, and so the expansion of polymeric network was restricted, and the swelling capabilities of the superabsorbents were remarkably decreased.

Effects of Surfactant Solutions on Water Absorption

For evaluating the effect of ionic surfactants on the swelling behavior of GG-*g*-PNaA/MS superabsorbent composite, the equilibrium water absorption of the composite in SDS and DTAB solution was determined and is shown in Fig. 8. It was observed that the water absorption is mainly dependent on the charge and concentration of surfactant. The water absorption of the composite decreased with an increase in the concentration of surfactant, but the decreasing tendency in DTAB solution is more obvious than that in SDS solution. The equilibrium water absorption of the composite in DTAB solution is always lower than that in SDS solution at the concentration higher than 0.1 mmol/L; the water absorption is close to zero in DTAB solution but reaches 207 g/g in SDS solution at 10 mmol/L. As an anionic superabsorbent, the negatively charged $—COO^-$ groups of the composite form strong association, binding or interaction with positively charged DTAB molecules, and the —COOH groups may also form strong hydrogen bonding interaction with quaternary ammonium cations of DTAB. In addition, the surfactant molecules may form aggregation within or over the networks of composites, which greatly decreased the hydrophilicity of polymer network and decreased the water absorption [35]. These factors are responsible for the faster decreasing rate and lower swelling capacity of the composite in DTAB solution. In anionic surfactant SDS, the negatively charged $—COO^-$ groups produce strong repulsion to the anions of the polymeric chains, the SDS molecules is hardly to enter the network of superabsorbent composite. As a result, the composite showed a comparatively higher water absorption in the anionic surfactant solution than in cationic surfactant solution.

Effects of Dye Solutions on Water Absorption

In this section, effects of the aqueous solutions of cationic and anionic dyes on the swelling properties of the composite were evaluated and are shown in Fig. 9. As can be seen, the water absorption decreased with increasing the concentration of dye solution. In the concentration range lower than 1 mmol/L, the water absorption of the composite in Methylene Blue solution is higher than that in Congo Red solution. However, a rapid deswelling occurred in Methylene Blue solution, but no similar tend-

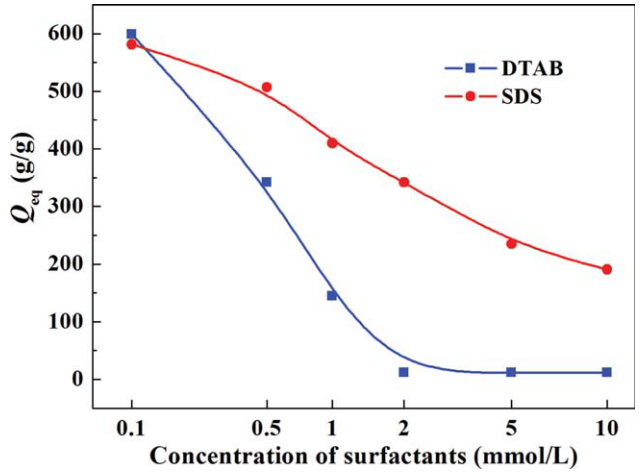

FIG. 8. Effect of surfactant solutions on the water absorption. [Color figure can be viewed in the online issue, which is available at wileyonlinelibrary.com.]

DOI 10.1002/pc

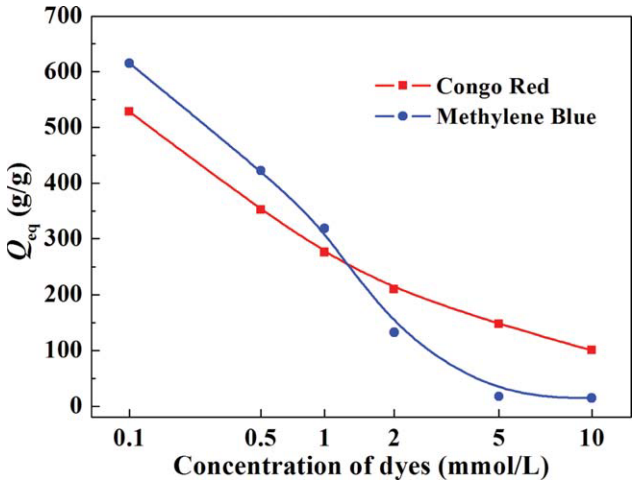

FIG. 9. Effect of dye solutions on the water absorption. [Color figure can be viewed in the online issue, which is available at wileyonlinelibrary.com.]

ency was observed in Congo Red solution when the concentration is larger than 1 mmol/L, and the water absorption in Methylene Blue solution is lower than that in Congo Red solution in this region. At the concentration of 10 mmol/L, the water absorption of the composite is only 15 g/g in Methylene Blue solution, but achieved 101 g/g in Congo Red solution, because Methylene Blue is a cationic dye. It can be easily adsorbed on the surface or entered the internal gel network of anionic superabsorbent composite. On the one hand, the $—COO^-$ groups on polymer chains were screened, and the expansion of network void was restricted because of the strong electrostatic and hydrogen-bonding interaction; on the other hand, the entrance of Methylene Blue into the gel network form additional crosslinking, and so the gel network collapsed. However, the anionic dye Congo Red is hardly to be attracted by the superabsorbent network because of the repulsion of same-charged ions, and only small amount of Congo Red can enter network through expansion-adsorption of 3-D network and hydrogen-bonding interaction. Figure 10 represents the FTIR spectra of the composites after swelling in Congo Red and Methylene Blue solutions. The C=C stretching vibration bands in the phenyl rings of Congo Red at 1,625 cm^{-1} appeared in the spectrum of composite after swelling in Congo Red solution (10 mmol/L) with a weakened intensity but shifted to 1,619 cm^{-1}. This indicates that only little Congo Red existed in the polymer network by hydrogen bonding interaction. Different from the situation for Congo Red, the characteristic absorption bands of Methylene Blue can be observed in the spectra of composite loaded Methylene Blue with greater intensity, and the —COOH absorption band of GG-*g*-PNaA/MS at 1,717 cm^{-1} shifted to 1,711 cm^{-1}. This revealed that large amount of Methylene Blue was adsorbed on the composite, and a hydrogen-bonding interaction occurred in this process.

CONCLUSIONS

New kinds of superabsorbent composites based on natural guar gum and medicinal stone were prepared as a part of the efforts to reduce the excessive consumption of petroleum resources and the environmental impact resulting from industrial polymers. FTIR, SEM, and TGA showed that PNaA chains had been grafted onto GG backbone and MS participates in the polymerization

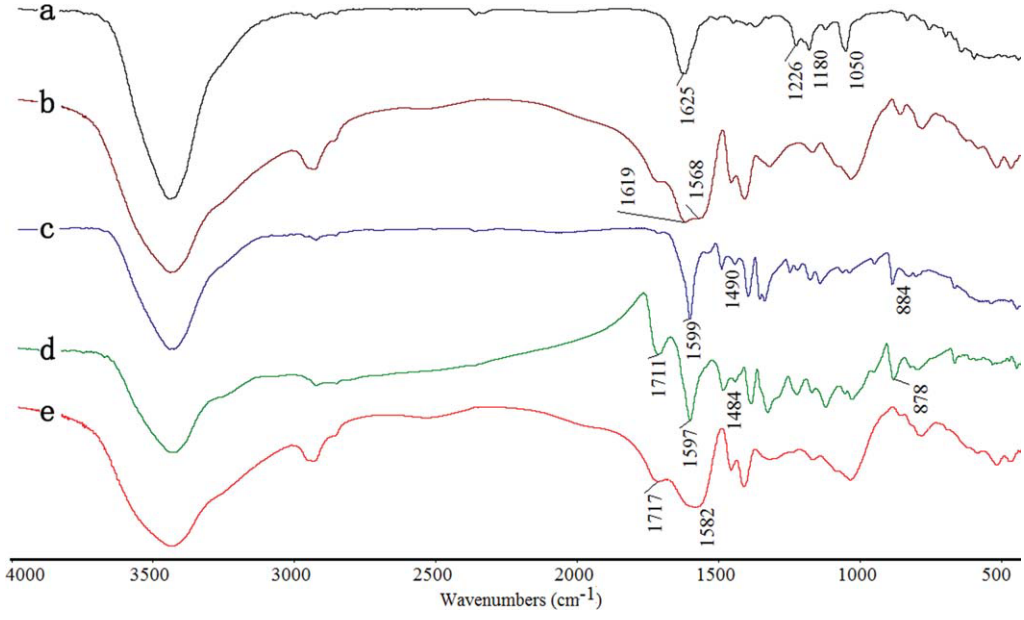

FIG. 10. FTIR spectra of (a) Congo Red, (b) GG-*g*-PNaA/MS after swelling in 10 mmol/L Congo Red solution, (c) Methylene Blue, (d) GG-*g*-PNaA/MS after swelling in 10 mmol/L Methylene Blue, and (e) GG-*g*-PNaA/MS. [Color figure can be viewed in the online issue, which is available at wileyonlinelibrary.com.]

through its active silanol groups, and the surface structure and thermal stability of the composite was improved by introducing MS. The incorporation of MS evidently enhanced the water absorption and swelling rate, and the water absorption increased by 96% than MS-free sample after incorporating 10 wt% MS. The superabsorbent composites process excellent pH-sensitivity and On–Off switching swelling characteristics between pH 7.2 and 2, which provided great possibility to extend the application domain of the composite. The superabsorbent composite showed distinct swelling behaviors in the saline solution with various valences, the surfactant, and dye solutions with various charges. The multivalent metal cations, cationic surfactant, and dye make the deswelling of gel network more rapid and obvious, whereas monovalent metal cation, anionic surfactant and dye only have less influence on the deswelling behavior. Therefore, the superabsorbent composites based on renewable, biodegradable, and nontoxic GG and MS showed improved water absorption capability and rate, as well as excellent pH responsibility, which can be used as potential water-manageable materials for various applications.

ACKNOWLEDGMENTS

This work was financially supported by the Western Action Project of CAS (No. KGCX2-YW-501) and "863" Project of the Ministry of Science and Technology, P. R. China (No. 2006AA03Z0454 and 2006AA100215).

REFERENCES

1. L.A. Utracki, M. Sepehr, and E. Boccaleri, *Polym. Adv. Technol.*, **18**, 1 (2007).
2. P. Liu, *Appl. Clay Sci.*, **38**, 64 (2007).
3. X.H. Qi, M.Z. Liu, F. Zhang, and Z.B. Chen, *Polym. Eng. Sci.*, **49**, 182 (2009).
4. K. Kosemund, H. Schlatter, J.L. Ochsenhirt, E.L. Krause, D.S. Marsman, and G.N. Erasala, *Regul. Toxicol. Pharm.*, **53**, 81 (2008).
5. L. Wu and M.Z. Liu, *Polym. Adv. Technol.*, **19**, 785 (2008).
6. F. Puoci, F. Iemma, U.G. Spizzirri, G. Cirillo, M. Curcio, and N. Picci, *Am. J. Agric. Biol. Sci.*, **3**, 299 (2008).
7. A.T. Paulino, M.R. Guilherme, A.V. Reis, G.M. Campese, E.C. Muniz, and J. Nozaki, *J. Colloid Interf. Sci.*, **301**, 55 (2006).
8. H. Kaşgöz, A. Durmus, and A. Kaşgöz, *Polym. Adv. Technol.*, **19**, 213 (2008).
9. M.R. Guilherme, A.V. Reis, A.T. Paulino, A.R. Fajardo, E.C. Muniz, and E.B. Tambourgi, *J. Appl. Polym. Sci.*, **105**, 2903 (2007).
10. Q.W. Tang, J.M. Lin, J.H. Wu, and M.L. Huang, *Eur. Polym. J.*, **43**, 2214 (2007).
11. M. Sadeghi and H.J. Hosseinzadeh, *J. Bioact. Compat. Pol.*, **23**, 381 (2008).
12. S. Kiatkamjornwong, K. Mongkolsawat, and M. Sonsuk, *Polymer*, **43**, 3915 (2002).
13. G. Crini, *Prog. Polym. Sci.*, **30**, 38 (2005).
14. J.K. Francis Suh and H.W.T. Matthew, *Biomaterials*, **21**, 2589 (2000).
15. S.S. Ray and M. Bousmina, *Prog. Mater. Sci.*, **50**, 962 (2005).
16. P. Lanthong, R. Nuisin, and S. Kiatkamjornwong, *Carbohydr. Polym.*, **66**, 229 (2006).
17. A. Li, J.P. Zhang, and A.Q. Wang, *Bioresour. Technol.*, **98**, 327 (2007).
18. A. Pourjavadi and G.R. Mahdavinia, *Polym. Polym. Compos.*, **14**, 701 (2006).
19. Y.T. Xie, A.Q. Wang, and G. Liu, *Polym. Compos.*, **31**: 89 (2010).
20. J.P. Zhang, Q. Wang, and A.Q. Wang, *Carbohydr. Polym.*, **68**, 367 (2007).
21. A. Pourjavadi, H. Hosseinzadeh, and M. Sadeghi, *J. Compos. Mater.*, **41**, 2057 (2007).
22. S.B. Hua and A.Q. Wang, *Carbohydr. Polym.*, **75**, 79 (2009).
23. X. Ding, L. Li, P.S. Liu, J. Zhang, N.L. Zhou, S. Lu, S.H. Wei, and J. Shen, *Polym. Compos.*, **30**, 976 (2009).
24. M.R. Guilherme, A.V. Reis, S.H. Takahashi, A.F. Rubira, J.P.A. Feitosa, and E.C. Muniz, *Carbohydr. Polym.*, **61**, 464 (2005).
25. A. Pourjavadi and H. Ghasemzadeh, *Polym. Eng. Sci.*, **47**, 1388 (2007).
26. J. Li, P.Y. Zhang, Y. Gao, X.G. Song, and J.H. Dong, *Environ. Sci. Technol. (China)*, **31**(10), 63 (2008).
27. A. Li, A.Q. Wang, and J.M. Chen, *J. Appl. Polym. Sci.*, **92**, 1596 (2004).
28. J.H. Wu, J.M. Lin, G.Q. Li, and C.R. Wei, *Polym. Int.*, **50**, 1050 (2001).
29. K. Taunk and K. J. Behari, *J. Appl. Polym. Sci.*, **77**, 39 (2000).
30. Y.H. Huang, J. Lu, and C.B. Xiao, *Polym. Degrad. Stab.*, **92**, 1072 (2007).
31. J.P. Zhang, Y. Liu, and A.Q. Wang, *Polym. Compos.*, **31**, 691 (2010).
32. H. Schott, *J. Macromol. Sci. B*, **31**, 1 (1992).
33. S. Kiatkamjornwong, W. Chomsaksakul, and M. Sonsuk, *Radiat. Phys. Chem.*, **59**, 413 (2000).
34. W.F. Lee and R.J. Wu, *J. Appl. Polym. Sci.*, **62**, 1099 (1996).
35. Y.M. Mohan, T. Premkumar, D.K. Joseph, and K.E. Geckeler, *React. Funct. Polym.*, **67**, 844 (2007).

 DOI 10.1002/pc